https://doi.org/10.1021/acs.analchem.1c03611

Fragment Hit Discovery and Binding Site Characterization by Indirect Affinity Capillary Electrophoresis: Application to Factor XIIa

Clara Davoine[a,b], Alissia Pardo[b], Lionel Pochet[a,‡], Marianne Fillet[b,‡,*]

[a]Namur Medicine & Drug Innovation Center (NAMEDIC – NARILIS), University of Namur, Rue de Bruxelles 61, 5000 Namur, Belgium

[b]Laboratory for the Analysis of Medicines (LAM), Department of Pharmacy, CIRM, University of Liege, Avenue Hippocrate 15, B36 Tour 4 +3, 4000 Liège, Belgium

ABSTRACT: Fragment-based lead discovery is a usual strategy in drug discovery to identify innovative lead compounds. The success of this approach strongly relies on the capacity to detect weak binders and characterize their binding site. NMR and X-ray crystallography are the conventional technologies used to tackle this challenge. However, their large protein consumption and the cost of equipment reduce their accessibility. Here, an affinity capillary electrophoresis methodology was developed that enables the detection of mM binders, the determination of dissociation constants, and the characterization of the fragment binding site. On the basis of multiple equilibrium theory, dissociation constants in the µM-mM range were determined and a new methodology is proposed to establish graphically if two fragments bind the same protein pocket. The applicability of this methodology was demonstrated experimentally on coagulation factor XIIa by evaluating pairs of fragments with expected behavior. This study reinforces the significance of using affinity capillary electrophoresis to gather valuable information for medicinal chemistry projects.

In drug discovery, biophysical techniques are commonly used to analyze the binding of a compound to a target. Each technique has its own characteristics regarding the information generated, the requirements, and the ability to detect low affinity. The selection of the appropriate technique is based on the questions arising during drug discovery projects.[1] In the early phases, the main preoccupations concern the discovery of hits and the characterization of their binding site. During hit discovery, the technique has to determine the affinity for the target inside the desired dynamic range. Binding site characterization aims to locate the zone where the compound binds on the target.[1,2] Compared to high-throughput screening (HTS), the fragment-based lead discovery (FBLD) approach screens compounds of lower size (< 300 g/mol). These fragments have weaker affinity but explore more efficiently the chemical space. Hence, FBLD projects work successfully with libraries of 1000-2000 fragments. The biophysical method used to discover fragment hits requires sensitivity at the µM to mM levels.[3,4] Several techniques can reach low mM affinity, such as X-ray crystallography, microscale thermophoresis, and NMR methods. However, they require either or both high concentration of fragments and high consumption of protein.[1] Therefore, screening methods with low demand on fragment solubility are still needed to expand the diversity of fragments that can be screened.[4] Besides, X-ray crystallography and NMR approaches require expensive instruments.

In this context, indirect affinity capillary electrophoresis (iACE) should be considered as a valuable microfluidic biophysical technique for use in FBLD projects. Affinity capillary electrophoresis (ACE) records the change in electrophoretic mobility of an analyte upon interaction with the target. The methodology works without target modification in near-physiological media. Interestingly, it supports impure samples and the analysis of targets lacking biological activity.[5,6] These characteristics explain its increasing use for the validation of HTS results.[7] However, compounds have to form a ligand-target complex with distinctive electrophoretic mobility.[6] To overcome this constraint, an indirect mode, known as competitive ACE, was applied for dissociation constant (K_D) determination and screening purposes.[8–13] In this configuration, the effect of the analyte is indirectly evaluated by measuring the displacement of a known binder, called the reporter.[12]

This paper outlines experimental procedures to screen fragments, estimate K_D, and determine the mutual effect of two fragments on the target. The dynamic range of affinity accessible by iACE was investigated. Moreover, the multiple equilibrium theory was applied to those experimental conditions to gather valuable information for medicinal chemists.

In this work, coagulation factor XIIa (FXIIa) was selected as the target protein to illustrate this iACE methodology. FXIIa is a S1A serine protease implicated in coagulation, inflammation, and immunity.[14] This protease is the target of our ongoing medicinal chemistry program[15–17]. The potential indications of FXIIa inhibitors include artificial surface-induced thrombosis, hereditary angioedema, Alzheimer's disease, and multiple sclerosis.[14] Currently, our primary screening is a chromogenic assay. The results of the newly developed iACE method were compared to the ones obtained with this biochemical assay.

EXPERIMENTAL SECTION

Materials

Benzamidine (BZM), pentamidine isethionate, diminazene aceturate, poly(ethylene oxide) (PEO) (Mv 200,000), *N*-(pyridine-4-ylmethyl)guanidine (compound 2), 3-chlorobenzylamine (compound 4), L-arginine (compound 5), 4-guanidinobenzoic acid hydrochloride (compound 6), 4-(aminomethyl)piperidine (compound 7), *cis*-cyclohexane-1,4-diamine (compound

https://doi.org/10.1021/acs.analchem.1c03611

16), and L-pipecolic acid (compound 20) were purchased from Sigma-Aldrich (Saint-Louis, MO). *Para*-aminobenzamidine (PABZM), nitric acid compound with *N"*-phenylguanidine (1:1) (PhGu), 1-benzothiophene-3-carboximidamidine hydrochloride (NAMFrag66), and L-prolinamide (compound 13) were sourced from Acros Organics (Fair Lawn, NJ). 4-Amidinobenzamide hydrochloride (NAMFrag60) and 6-amidino-2-naphthol methanesulfonate (NAMFrag56) were acquired from TCI Europe (Zwijndrecht, Belgium). Life Chemicals (Ontario, Canada) provided 2-phenylacetamidoxime (compound 3). Phenobarbital (compound 9) was purchased from Fagron (Nazareth, Belgium). Piperidine-1,3-dicarboxamide (compound 10) was sourced from Vitas-M Laboratory, Ltd. (Causeway Bay, Hong Kong). BBV-93483954 (compound 1) and EN300-152798 (compound 15) were acquired from Enamine (New Jersey, USA). (2*R*,4*R*)-4-Methylpiperidine-2-carboxylic acid (compound 18) was obtained from ABCR GmbH (Karlsruhe, Germany). Compounds 8, 11, 12, 14, 17 and 19 were obtained from the chemical library developed within the Namur Medicine and Drug Innovation Center. Human plasma β-factor XIIa (FXIIa) in solution at 1.12 mg/mL was purchased from Molecular Innovations (Novi, MI). The physicochemical properties of the fragment library, such as aqueous solubility and global charge at pH 7.4, were computed by MarvinSketch 19.27 (ChemAxon Ltd., Budapest, Hungary).

Chromogenic FXIIa Assay

The chromogenic FXIIa assay and its data analysis were performed as reported by Davoine et al.[5] The assay was previously validated based on the requirements described by the National Center for Advancing Translational Sciences.[18]

Capillary Electrophoresis

A Hewlett Packard three-dimensional capillary electrophoresis system from Agilent Technologies (Waldbronn, Germany) operated by Agilent OpenLab CDS C.01.07 (27) software was used for this study. The method was adapted from Davoine et al.[5] Capillary electrophoresis was carried out using a buffer made of 21 mM Tris, 21 mM *N*-(2-hydroxyethyl)piperazine-N′-ethanesulfonic acid (HEPES), 81 mM NaCl, 1.6 mM sodium acetate, and 100 µM ethylenediaminetetraacetic acid (EDTA) (pH 7.4) at a constant voltage of –3 kV (generating a current of approximately 49 µA) with on-column detection at 262 ± 2 nm (using a reference wavelength at 360 ± 50 nm). EDTA suppressed the false-positive signal of metal-contaminated samples. The capillary (75 µm i.d.), provided by Polymicro Technologies, Inc. (Phoenix, AZ), was 33 cm in total length (8.5 cm from injection to detection) and PEO-coated.[5] FXIIa (15 µM) was introduced in the capillary by vacuum injection at –80 mbar for 0 or 12 s. Then, pentamidine (the reporter, 10 µM) was injected at –20 mbar for 5 s, followed by a short plug of background electrolyte (BGE).

Sample Preparations

The stock solution of FXIIa was 2.5-fold diluted with Tris-HEPES buffer (35 mM Tris, 35 mM HEPES, 35 mM NaCl, 167 µM EDTA, adjusted at pH 7.4 with 0.1 M phosphoric acid) containing 0.05% Tween 20 to reach the final concentration of 15 µM. Fragments were prepared at 20 mM in methanol and kept at –80°C. Methanol was evaporated at 35 °C until dryness using a Centrivap concentrator connected to a cold trap (Labconco, Kansas City, MO). The residue was dissolved in the Tris-HEPES buffer at an adequate concentration. The latter solution was used to introduce the fragment(s) in the BGE and the FXIIa-diluting buffer.

Data Treatment

The data treatment was similar to the study by Davoine et al.[5] The migration time was determined by CEVal software version 0.6h9[19] using the Haarhoof–Van der Linde fit to take into account peak distortion. The shift inhibition (%) was calculated by equation 1, which was derived from Farças et al.[10] Compared to the latter, equation 1 introduces the migration time of the reporter in the fragment-containing BGE without the loaded protein ($M_{t,Fg}$).

$$Shift\ inhibition = \left(1 - \left(\frac{M_{t,C} - M_{t,Fg}}{M_{t,T} - M_{t,BGE}}\right)\right).100 \qquad (Eq.1)$$

where $M_{t,T}$ is the migration time of the reporter with the loaded protein in pure BGE (min), $M_{t,C}$ is the migration time of the reporter with the loaded protein in the fragment-containing BGE (min), $M_{t,BGE}$ is the migration time of the reporter without the loaded protein in pure BGE (min), and $M_{t,Fg}$ is the migration time of the reporter without the loaded protein in the fragment-containing BGE (min).

Statistical analysis was made with Microsoft Office Excel 2016 (Microsoft, Redmond, WA). The equations used for the K_D estimation and mutual effect determination are discussed in the text. Regressions (linear and non-linear) were performed by GraphPad Prism version 9.0.0 (121) (San Diego, CA).

RESULTS AND DISCUSSION

Previously, a partial-filling direct ACE method with FXIIa as the target was developed by our team and confirmed its applicability for K_D determination and hit cross-validation.[5] This method is limited to binders in the µM range that are positively charged and UV–vis absorbent.[5] The present project aimed to design an indirect version of the latter to expand fragments' diversity and detect weaker interactions.

Optimization of the iACE Method

First, the reporter molecule was selected based on the following criteria: (1) low µM affinity, (2) fast equilibrium behavior, (3) UV–vis absorbance, and (4) stability in solution for at least 5 h. Pentamidine meets all these criteria and has an absorption maximum determined at 262 nm. In the initial settings, an important shift of 20.0 ± 0.1 min was observed when a FXIIa plug of 19.6 cm was applied. To reduce the analysis time and improve the reporter's signal, short-end injection was performed and the method was adapted.[20] With a short FXIIa plug of 5.6 cm, a shift of 6.7 ± 0.1 min was observed and considered sufficient. The BGE buffer capacity was also enhanced to support the incorporation of mM concentrations of additives (See Table S1). Indeed, insufficient buffer capacity associated with low volume reservoirs (200 µl) favor the change of pH in the anodic reservoir by anion accumulation during electrophoresis.[21] Alterations of the pH can affect the migration times, the binding, and the PEO coating.[21]

Applicability of iACE for Fragment Hit Discovery

To evaluate the assay performances, six reference compounds were first selected across the µM-mM range of affinity based on our previous study.[5] Then, the lowest detectable affinity was estimated according to the fragment concentration (150–600 µM) added in the BGE (See Figure 1 and Table S2). PhGu was also evaluated at a higher concentration (3000 µM)

https://doi.org/10.1021/acs.analchem.1c03611

to determine if such a low-affinity binder can be detected (estimated K_i = 7.3 ± 0.3 mM). Figure 1 depicts their respective shift inhibition percentage. The critical point was to set the threshold in shift inhibition percentage that was necessary to tag the compound as a binder or not. Relative standard deviation (RSD) of the shift inhibition percentage was calculated at 6.2% using Eq. 1; considering the variability of the control runs with (24 measures, RSD 2.4%) and without FXIIa (308 measures, RSD 2.9%), two thresholds were set at 12.4% (2-fold the RSD value; Th_1) and at 18.6% (3-fold the RSD value; Th_2). The tested compounds were considered as potential binders or binders when above 12.4 or 18.6%, respectively. As shown in Figure 1, higher fragment concentration in the BGE allowed the detection of weaker interactions. Consequently, for screening applications, the desired detectable affinity range can be easily adapted by changing the fragment concentration in the BGE. Interestingly, a significant displacement of the reporter occurred at a lower concentration than their respective K_D. Indeed, to attain Th_1 or Th_2, the fragment concentration in the BGE has to be 0.3-fold or 0.4-fold the K_D, respectively. So, even a low occupancy of the protein binding sites allows the detection of the binding, as it is the case in NMR.[1] This characteristic is an asset compared to methods that need a fragment concentration around or over the K_D, such as most of the biochemical assays (around the K_D), X-ray crystallography (over the K_D), and microscale thermophoresis (5–10 times the K_D).[1,3]

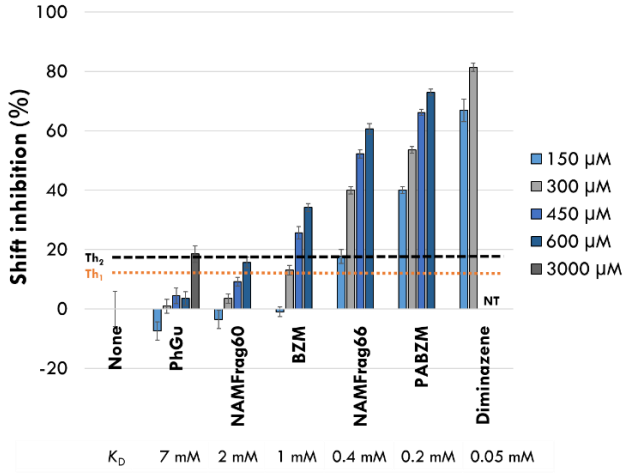

Figure 1. Shift inhibition (%) of the references at different concentrations. K_D: dissociation constant, NT: not tested, Th_1: threshold for potential binders (12.4%), and Th_2: threshold for binders (18.6%).

In a screening context, the analysis throughput is an important parameter that could limit the size of the tested library. To improve the throughput of our iACE method, the screening of fragments in mixtures could be considered. The potential impact of those mixtures on the current and on the measured shift inhibition for each fragment had to be investigated. According to Chu et al.,[8] the total concentration of additives that can be added to the BGE is usually 10% of the buffer's concentration. An overall concentration of fragments at 3 mM concentration was used for the assay in mixtures. Three known binders (PhGu, BZM, and NAMFrag66) with different affinity levels and 17 nonbinders displaying various ionization states were selected (Table S4). A nonbinder was defined by an inhibition inferior to 5% at 1 mM or 10% at ≥ 3 mM in the chromogenic FXIIa assay. The concentrations for the fragments were 600 µM, and each tested mixture contained one binder and four nonbinders. The first set of experiments (mix 1) was designed as a worst-case scenario with five fully charged fragments. As can be seen in Table S3, no significant change in pH, current, and shift inhibition was noticed. Indeed, only a slight increase of 0.2, 4.0, and 1.8% was observed for PhGu, BZM, and NAMFrag66, respectively. The impact of various nonactive fragments possessing different charge states (see Table S4, mix 2–4) was also evaluated by preparing random mixtures containing four nonbinders and one binder. In all cases, screening in mixtures did not generate false negatives or significant change in the current or shift inhibition measurement (see Table S3). No impact of the charge state of the fragments on the results was observed under the optimized conditions, allowing the analysis of positively, negatively, and noncharged compounds. It is worth noting that the number of compounds that can be included in a mixture depends on the overall concentration of fragments and thus on the desired lowest detectable affinity.

Determination of Dissociation Constants

Screenings are usually performed at a single concentration. However, to determine K_D and to validate that the hits behave adequately in a dose-dependent manner, several concentrations have to be tested. To calculate the K_D of the tested fragments by iACE, a general equilibrium binding model was used (see Scheme 1). Accordingly, the macromolecule (E) is allowed to form a complex with the reporter (R), the fragment (Fg), or both, leading to E·R, E·Fg, or E·R·Fg, respectively. The model assumed that R·Fg is not formed, that no other type of interaction takes place, and that the binding stoichiometry is 1:1. For binary complexes, K_D's are symbolized as K with the compound that dissociates as a subscript. The K_D's of the ternary complex are symbolized as K' with the compound that dissociates as a subscript.

$$\begin{array}{ccc} E & \overset{K_R}{\leftrightharpoons} & E \cdot R \\ {\scriptstyle K_{Fg}}\,\uparrow\downarrow & & \downarrow\uparrow\,{\scriptstyle K'_{Fg}} \\ E \cdot Fg & \underset{K'_R}{\rightleftharpoons} & E \cdot R \cdot Fg \end{array}$$

Scheme 1. Equilibria among the Protein Species in the Presence of the Reporter and a Fragment

Under rapid-equilibrium conditions, the reporter's bound fraction (r) for the above mechanism can be described by Eq. 2.[22]

$$r = \frac{[R]\left(1 + \frac{[Fg]}{K'_{Fg}}\right)}{K_R\left(1 + \frac{[Fg]}{K_{Fg}}\right) + [R]\left(1 + \frac{[Fg]}{K'_{Fg}}\right)} \qquad (Eq.\,2)$$

where r is the reporter's bound fraction, *[R]* is the reporter concentration, *[Fg]* is the fragment concentration, K_R is the dissociation constant of the reporter, K_{Fg} is the dissociation constant of the fragment, and K'_{Fg} is the dissociation constant of the fragment from the E·R·Fg complex.

With competitive binders, the E·R·Fg complex is not formed, and the reporter's bound fraction is described by Eq. 3.[22]

$$r = \frac{[R]}{K_R\left(1 + \frac{[Fg]}{K_{Fg}}\right) + [R]} \qquad (Eq.\,3)$$

The rearrangement of Eq. 3 into a linear function of *[Fg]* leads to Eq. 4.

https://doi.org/10.1021/acs.analchem.1c03611

$$\left(\frac{1}{r}-1\right)=\frac{K_R}{[R]}\left(1+\frac{[Fg]}{K_{Fg}}\right) \qquad (Eq.4)$$

Eq. 4 indicates that, if $\left(\frac{1}{r}-1\right)$ is plotted against *[Fg]*, a straight line is obtained with a slope of $\frac{K_R}{[R]K_{Fg}}$, a *y*-axis intercept at $\frac{K_R}{[R]}$, and an *x*-axis intercept at $-K_{Fg}$.

In our iACE configuration, the reporter bound fraction can be calculated by Eq. 5 (See Supporting Information—Supplemental Data—2.1).

$$r=\frac{M_{t,R}-M_{t,P}}{(1-x)M_{t,R}-M_{t,P}} \qquad (Eq.5)$$

where *x* is the fraction of the effective capillary length that is filled with the target plug, $M_{t,R}$ is the migration time of the reporter without the target plug, and $M_{t,P}$ is the migration time of the reporter with the target plug.

For K_D determination of the references, several concentrations were tested. As expected, a larger compound's concentration in the BGE generated a larger reduction of the reporter migration time (see Figure S1). Eq. 5 calculated the reporter's bound fraction. Then, the reporter's bound fractions of different fragment concentrations were fitted to the two binding mechanisms (noncompetitive and competitive, Eq. 2 and 3). The extra sum-of-squares F test (*P*-value of 0.05) selected the model. The K_D of each reference is shown in Table 1. The K_D's obtained by iACE were similar to their respective inhibition constant (K_i) that were previously reported in the literature (PABZM and BZM)[5,23] or estimated by the Cheng–Prusoff equation for competitive inhibitors (diminazene, NAMFrag66, NAMFrag60). Indeed, the overall minimum significant ratio (MSR) of the chromogenic assay was assessed at 1.3 using a control compound (see Supporting Information—Supplemental Data—1). Control compound MSR tends to be optimistic because it is based on a single well-behaved compound.[24] In consequence, a potency ratio between 0.7 and 1.5 was not considered significantly different in our FXIIa medicinal chemistry program (see Table 1). FXIIa concentration is a critical parameter that can affect the K_D determination. Generally, to avoid an effect of the protein concentration on the binding equilibrium, the ratio K_D on FXIIa concentration has to be at least equal to 10.[25] The chromogenic assay and the iACE were performed at a FXIIa concentration of 14 nM and 15 µM, respectively. It means that the iACE method described in this paper is more suited for the determination of K_D superior to 150 µM.

Figure 2 shows the nonlinear and linear regressions of the different tested compounds. Because the *x*-intercept of the linear function is equal to $-K_{Fg}$, this plot could be used to display the data, especially when the objective is to show relative differences in K_D.

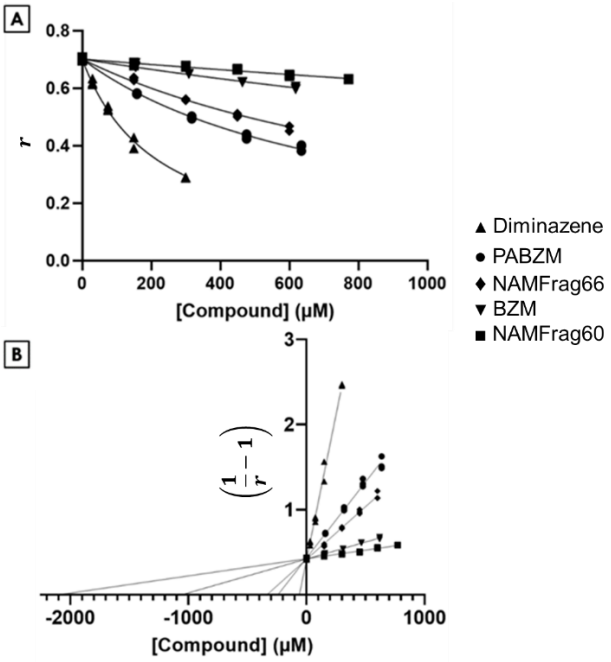

Figure 2. Determination of the dissociation constant of diminazene, PABZM, NAMFrag66, BZM, and NAMFrag60: (A) nonlinear regression plot, and (B) linear regression plot. BZM: benzamidine, [compound]: concentration of compound added in the BGE, *r*: reporter bound fraction, and PABZM: *p*-aminobenzamidine.

Characterization of the Fragment Binding Site

To facilitate the hit optimization phase in drug discovery, the binding site has to be characterized. Displacement assays, such as the iACE described in this paper, can be used for this purpose as a rapid test when the reporter binding site is well identified.[1] When working with S1A serine proteases in a FBLD context, the main question is to determine if the fragment binds the S1 pocket or not (see Figure S2A). The S1 pocket is known to drive the major part of the association energy.[14] S1 binders tend to be more potent than non-S1 binders. Thus, a fragment hit selection only based on potency will result in numerous S1 binders. Linking S1 binders between them will not be relevant for the design of a larger molecule.

Table 1. Determination of the Dissociation Constants (K_D)

Compound	Chromogenic assay	Indirect ACE assay		K_D/K_i ratio
	$K_i \pm S_D$ (µM)	K_D (CI) (µM)	Model	
Diminazene	49.3[b] (± 1.4)	64.94 (62.04-67.99)	Competitive	1.3
PABZM	163.2[a] (± 0.5)	234.7 (228.3-241.3)	Competitive	1.4
NAMFrag66	379[b] (± 9)	354.1 (341.3-367.6)	Competitive	0.9
BZM	1032[b,c] (± 37)	1110 (1057-1168)	Competitive	1.1
NAMFrag60	1611[b] (± 121)	2162 (2049-2288)	Competitive	1.3
PhGu	7335[b] (± 290)	ND	ND	NA

[a] Previously reported[5] [b] Estimated by the Cheng–Prusoff equation for competitive inhibitors [c] Reported by Tans et al.[23] at 1.12 mM (pH 7.2) K_i: inhibitory constant, S_D: standard deviation, CI: confidence interval of 95%, NA: not applicable, and ND: not determined.

https://doi.org/10.1021/acs.analchem.1c03611

To determine if the binder is located in the S1 pocket, the more convenient experiment would be to use BZM as the reporter instead of pentamidine (see Figure S2B and C). Indeed, BZM was co-crystallized in the FXIIa S1 pocket.[26] If the fragment can displace BZM, this means that the fragment binds the S1 pocket (Figure S2C); but in our configuration, BZM cannot be used as the reporter because its affinity for FXIIa is too weak. Indeed, no shift in the migration time of BZM was observed when a plug of FXIIa was applied. To overcome this problem, a cross-competition ACE assay was investigated.

With this in mind, a general equilibrium binding model was constructed to evaluate the mutual exclusivity of two fragments (see Scheme 2). In this model, the macromolecule (E) is allowed to form a complex with the reporter (R), fragment 1 (Fg_1), fragment 2 (Fg_2), or the two fragments, leading to E·R, E·Fg_1, E·Fg_2, or E·Fg_1·Fg_2, respectively. The model assumes that R·Fg, E·R·Fg_1, and E·R·Fg_2 are not formed, that no other type of interaction takes place, and that the binding stoichiometry is 1:1.

$$E \cdot R \overset{K_R}{\leftrightharpoons} E \overset{K_{Fg1}}{\leftrightharpoons} E \cdot Fg_1$$
$$K_{Fg2} \,\downarrow\uparrow \qquad \downarrow\uparrow\, \alpha.K_{Fg2}$$
$$E \cdot Fg_2 \underset{\alpha.K_{Fg1}}{\rightleftharpoons} E \cdot Fg_1 \cdot Fg_2$$

Scheme 2. Equilibria among the Protein Species in the Presence of the Reporter and Two Fragments

Under rapid-equilibrium conditions, the bound reporter fraction (r) for the above mechanism can be described by Eq. 6 (see Supporting Information—Supplemental Data—2.2).

$$r = \frac{[R]}{K_R\left(1 + \frac{[Fg_1]}{K_{Fg1}} + \frac{[Fg_2]}{K_{Fg2}} + \frac{[Fg_1].[Fg_2]}{\alpha.K_{Fg1}.K_{Fg2}}\right) + [R]} \quad (Eq.6)$$

where $[Fg_1]$ is the Fg_1 concentration, $[Fg_2]$ is the Fg_2 concentration, K_{Fg1} is the dissociation constant of Fg_1, K_{Fg2} is the dissociation constant of Fg_2, and α is the interaction constant between Fg_1 and Fg_2 in the E·Fg_1·Fg_2 complex. When Fg_1 and Fg_2 interact at the same site, they are mutually exclusive, the E·Fg_1·Fg_2 complex cannot be formed, and thus $\alpha = \infty$. If Fg_1 and Fg_2 interact with different sites, the E·Fg_1·Fg_2 complex is formed and $\infty > \alpha > 0$.

The rearrangement of Eq. 6 into a linear function of $[Fg_1]$ leads to Eq. 7.

$$\left(\frac{1}{r} - 1\right) = \frac{K_R}{[R]}\left(1 + \frac{[Fg_1]}{K_{Fg1}} + \frac{[Fg_2]}{K_{Fg2}} + \frac{[Fg_1].[Fg_2]}{\alpha.K_{Fg1}.K_{Fg2}}\right) \quad (Eq.7)$$

Eq. 7 indicates that, if $\left(\frac{1}{r} - 1\right)$ is plotted against $[Fg_1]$ at fixed $[Fg_2]$, a straight line will be obtained with a slope of

$$\frac{K_R.\left(1 + \frac{[Fg_2]}{\alpha.K_{Fg2}}\right)}{[R].K_{Fg1}}$$

a y-axis intercept at

$$\frac{K_R.\left(1 + \frac{[Fg_2]}{K_{Fg2}}\right)}{[R]}$$

and an x-axis intercept at

$$-K_{Fg1}.\frac{\left(1 + \frac{[Fg_2]}{K_{Fg2}}\right)}{\left(1 + \frac{[Fg_2]}{\alpha.K_{Fg2}}\right)}$$

Similar to the Yonetani–Theorell analysis[27] used to treat kinetic data, the y-intercept is a linear function of $[Fg_2]$ independent of the α value. In the case of mutually exclusive binders ($\alpha = \infty$), the slope is constant $\left(= \frac{K_R}{[R]K_{Fg1}}\right)$, meaning that plots of $\left(\frac{1}{r} - 1\right)$ versus $[Fg_1]$ at diverse $[Fg_2]$ generates parallel straight lines. The cut-off for mutually exclusive binding is generally set at $\alpha > 10$.[28] In the case of nonmutually exclusive binders ($\infty > \alpha > 0$), both the slope and the y-axis intercept of the plots $\left(\frac{1}{r} - 1\right)$ versus $[Fg_1]$ become linear functions of $[Fg_2]$. The straight lines obtained in the presence and absence of Fg_2 intersect at an abscissa value of $-\alpha K_{Fg1}$. Thus, the α value can be calculated from this intersection. Indeed, K_{Fg1} can be independently determined using the data generated in the absence of Fg_2 (see Section—Determination of Dissociation Constants). Moreover, depending on the α value, one can assess if the binding of the two fragments in the E·Fg_1·Fg_2 complex is synergistic ($1 > \alpha > 0$), independent ($\alpha = 1$), or antagonistic ($\infty > \alpha > 1$).

To demonstrate the applicability of this graphical method, two pairs of fragments were selected, one being mutually exclusive (BZM and PABZM) and the other being non-mutually exclusive (NAMFrag56 and PhGu—See Figure 3).

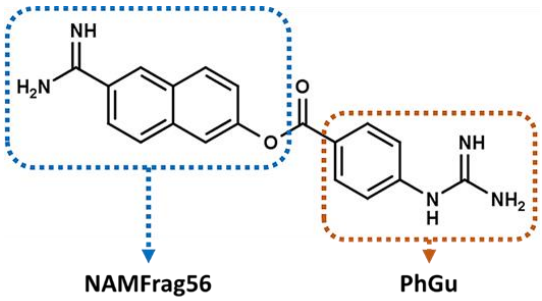

Figure 3. Structure of nafamostat. The boxes delimit the non-mutually exclusive fragments obtained after fragmentation of a FXIIa inhibitor.

BZM was co-crystallized in the FXIIa S1 pocket (PDB: 6B74).[26] PABZM was chosen on the basis of its similarity to BZM (Tanimoto value of 0.9[29]) and the fact that it was co-crystallized in the S1 pocket of other S1A serine proteases such as kallikrein (PDB: 2BDG),[30] thrombin,[31] and FVIIa (PDB: 2A2Q).[32] The mutual exclusivity of BZM and PABZM was confirmed by Yonetani–Theorell analysis (see Figure 4A) and by iACE (see Figure 4C) using our original procedure. Then, NAMFrag56 and PhGu were used as nonmutually exclusive binders since these compounds result from the fragmentation of nafamostat, a potent FXIIa inhibitor[14] (see Figure 3). The non-mutual exclusivity of NAMFrag56 and PhGu was obtained by Yonetani–Theorell analysis and iACE (see Figure 4B and D), which confirmed the validity of our methodology. It is worth noting that, in contrast to the Yonetani-Theorell analysis,[27] our iACE approach is a pure binding assay that does not rely on biological activity.

https://doi.org/10.1021/acs.analchem.1c03611

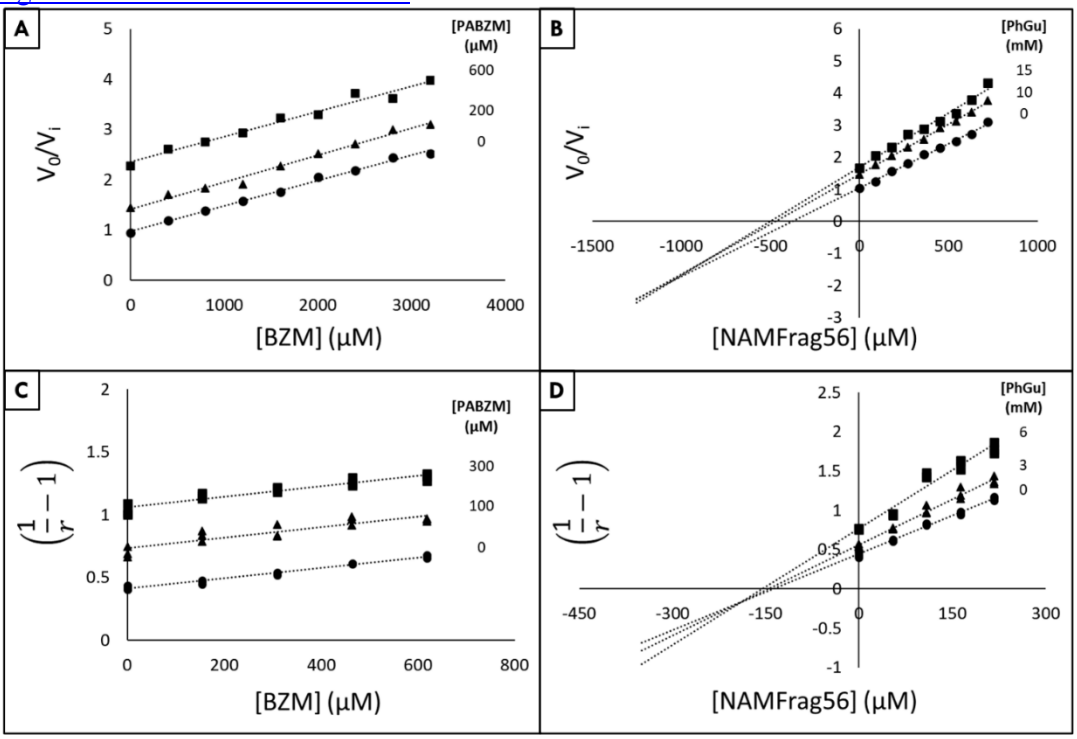

Figure 4. Mutual effect of two fragments on FXIIa by the Yonetani–Theorell analysis (plots A and B) and the present procedure (plots C and D). [BZM]: concentration of benzamidine, [NAMFrag56]: concentration of 6-amidino-2-naphthol, [PABZM]: concentration of *p*-aminobenzamidine, [PhGu]: concentration of phenylguanidine, *r*: reporter's bound fraction, V_0: initial reaction rate with the vehicle, and V_i: initial reaction rate with fragment(s).

CONCLUSION

The iACE methodology reported in this paper provides an efficient approach for the early phases of drug discovery projects. The technology can be used for the detection of weak interactions, K_D determination, and binding site characterization. This technique constitutes an extension to the FBLD analytical toolbox that already includes NMR, X-ray crystallography, thermal shift, surface plasmon resonance, microscale thermophoresis, differential static light scattering,[3,33] and DNA-encoded chemical libraries.[34–37] Neither biological activity nor modification of the target is required. However, a known ligand with low µM affinity and fast kinetics is needed. The reporter's electrophoretic mobility has to be distinctive from the target's one, and its chromophore has to be chosen properly to minimize spectrophotometric interferences. The tested fragments should not have an absorbance close to the detection wavelength. The maximal number of fragments that can be screened simultaneously corresponds to 10% of the buffer's concentration divided by 0.3-fold the lowest desired detectable affinity. The target must not interact with the silica wall or the BGE's components. The conductivity and viscosity of the target plug must also be similar to the rest of the capillary filled with BGE.

Nonspecific binding such as "selective promiscuous binders"[38] (e.g., binding of cationic fragments around negatively charged proteins) is unlikely. In addition, tight binders do not generate false negatives in contrast to the ligand-based NMR.[8,38] Still, the switch of the direct ACE mode to the indirect leads to a loss of the separative character. The binding of a fragment in an allosteric site can also induce active-site reporter displacement. So, the displacement of the reporter does not systematically mean that the fragment enters into a competition with the reporter. For this reason, the term "competitive ACE" should be avoided. Moreover, the protein is incubated with the fragment. This means that the protein can be trapped by aggregators, or denatured by reactive compounds.[38–41] However, the latter is a common pitfall of biophysical techniques. Stable and nonaggregating compounds under the given experimental conditions are a prerequisite to obtain accurate results.[1]

Regarding hit discovery, iACE detects interaction at low occupancy of the protein binding site (< 30%) and, if the protein and the detection of the reporter tolerate it, could operate with DMSO.[42] Thus, the technique is less constrained by the fragment solubility. It demonstrates its ability to successfully determine K_D in the µM-mM range. The remaining drawback of the actual workflow is the throughput (15 fragments per day and instrument, including QCs and replicates), which is unsuitable for large-scale screening. However, an automated capillary electrophoresis instrument adapted for 96-well plates[43] could address this issue and run a library of 1000 fragments in a day. Finally, the iACE methodology can be adapted for the cross-competition assay to characterize fragment binding sites. A graphical diagnostic of the mutual exclusivity of two compounds, similar in concept to Yonetani–Theorell analysis, can be obtained thanks to the mathematical developments described in this paper. This graphical method could be suited for any technique that follows the assumed equilibrium binding model and reports the reporter bound fraction.

ASSOCIATED CONTENT

Supporting Information

The Supporting Information is available free of charge on the ACS Publications website.

https://doi.org/10.1021/acs.analchem.1c03611

Estimation of the overall minimum significant ratio for the chromogenic assay, full mathematical developments, and additional data, including electropherograms, fragments' structure, and representations of the β-FXIIa active site. (PDF)

AUTHOR INFORMATION

Corresponding Author

* E-mail address: marianne.fillet@uliege.be

Author Contributions

The manuscript was written through contributions of all authors. ‡These authors contributed equally.

ACKNOWLEDGMENT

C. D. received funding from the National Fund for Scientific Research (FNRS) Grant 40000455 and Fondation Léon Frédéricq Grant 2020-2021-30-C.F.F. L. P. received funding from the University of Namur FSR Grant L.POCHET-12/2021. M. F. received funding from the University of Liège Fonds Spéciaux—Crédits facultaires ID 14758.

We gratefully acknowledge the contribution of the following colleagues: Alice Demelenne and Marie-Jia Gou for their technical assistance with the capillary electrophoresis instrument.

REFERENCES

(1) Renaud, J. P.; Chung, C. W.; Danielson, U. H.; Egner, U.; Hennig, M.; Hubbard, R. E.; Nar, H. Biophysics in Drug Discovery: Impact, Challenges and Opportunities. *Nat. Rev. Drug Discov.* **2016**, *15* (10), 679–698. https://doi.org/10.1038/nrd.2016.123.

(2) Holdgate, G.; Geschwindner, S.; Breeze, A.; Davies, G.; Colclough, N.; Temesi, D.; Ward, L. Biophysical Methods in Drug Discovery from Small Molecule to Pharmaceutical. In *Protein-Ligand Interactions*; Williams, M. A., Daviter, T., Eds.; Methods in Molecular Biology; Humana Press: Totowa, NJ, 2013; Vol. 1008, pp 327–355. https://doi.org/10.1007/978-1-62703-398-5_12.

(3) Lamoree, B.; Hubbard, R. E. Current Perspectives in Fragment-Based Lead Discovery (FBLD). *Essays Biochem.* **2017**, *61* (5), 453–464. https://doi.org/10.1042/EBC20170028.

(4) Konteatis, Z. What Makes a Good Fragment in Fragment-Based Drug Discovery? *Expert Opin. Drug Discov.* **2021**, *00* (00), 1–4. https://doi.org/10.1080/17460441.2021.1905629.

(5) Davoine, C.; Fillet, M.; Pochet, L. Capillary Electrophoresis as a Fragment Screening Tool to Cross-Validate Hits from Chromogenic Assay: Application to FXIIa. *Talanta* **2021**, *226*, 122163. https://doi.org/10.1016/j.talanta.2021.122163.

(6) Farcas, E.; Pochet, L.; Crommen, J.; Servais, A.; Fillet, M. Capillary Electrophoresis in the Context of Drug Discovery. *J. Pharm. Biomed. Anal.* **2017**, *144*, 195–212. https://doi.org/10.1016/j.jpba.2017.02.022.

(7) Olabi, M.; Stein, M.; Wätzig, H. Affinity Capillary Electrophoresis for Studying Interactions in Life Sciences. *Methods* **2018**, *146* (May), 76–92. https://doi.org/10.1016/j.ymeth.2018.05.006.

(8) Chu, Y. H.; Avila, L. Z.; Biebuyck, H. A.; Whitesides, G. M. Using Affinity Capillary Electrophoresis to Identify the Peptide in a Peptide Library That Binds Most Tightly to Vancomycin. *J. Org. Chem.* **1993**, *58* (3), 648–652. https://doi.org/10.1021/jo00055a017.

(9) Austin, C.; Pettit, S. N.; Magnolo, S. K.; Sanvoisin, J.; Chen, W.; Wood, S. P.; Freeman, L. D.; Pengelly, R. J.; Hughes, D. E. Fragment Screening Using Capillary Electrophoresis (CEfrag) for Hit Identification of Heat Shock Protein 90 ATPase Inhibitors. *J. Biomol. Screen.* **2012**, *17* (7), 868–876. https://doi.org/10.1177/1087057112445785.

(10) Farcaş, E.; Hanson, J.; Pochet, L.; Fillet, M. Capillary Electrophoretic Mobility Shift Displacement Assay for the Assessment of Weak Drug-Protein Interactions. *Anal. Chim. Acta* **2018**, *1034*, 214–222. https://doi.org/10.1016/j.aca.2018.06.024.

(11) Pierceall, W. E.; Zhang, L.; Hughes, D. E. Affinity Capillary Electrophoresis Analyses of Protein–Protein Interactions in Target-Directed Drug Discovery. In *Protein-Protein Interactions. Methods in Molecular Biology, vol 261*; Fu, H., Ed.; Humana Press: New Jersey, 2004; pp 187–198. https://doi.org/10.1385/1-59259-762-9:187.

(12) Colton, I. J.; Carbeck, J. D.; Rao, J.; Whitesides, G. M. Affinity Capillary Electrophoresis: A Physical-Organic Tool for Studying Interactions in Biomolecular Recognition. *Electrophoresis* **1998**, *19* (3), 367–382. https://doi.org/10.1002/elps.1150190303.

(13) Nilsson, M.; Johansson, G.; Isaksson, R. Determination of Dissociation Constants by Competitive Binding in Partial Filling Capillary Electrophoresis. *Electrophoresis* **2004**, *25* (78), 1022–1027. https://doi.org/10.1002/elps.200305786.

(14) Davoine, C.; Bouckaert, C.; Fillet, M.; Pochet, L. Factor XII/XIIa Inhibitors: Their Discovery, Development, and Potential Indications. *European Journal of Medicinal Chemistry*. Elsevier Masson SAS December 15, 2020, p 112753. https://doi.org/10.1016/j.ejmech.2020.112753.

(15) Robert, S.; Bertolla, C.; Masereel, B.; Dogné, J.-M.; Pochet, L. Novel 3-Carboxamide-Coumarins as Potent and Selective FXIIa Inhibitors. *J. Med. Chem.* **2008**, *51* (11), 3077–3080. https://doi.org/10.1021/jm8002697.

(16) Bouckaert, C.; Serra, S.; Rondelet, G.; Dolušić, E.; Wouters, J.; Dogné, J.-M.; Frédérick, R.; Pochet, L. Synthesis, Evaluation and Structure-Activity Relationship of New 3-Carboxamide Coumarins as FXIIa Inhibitors. *Eur. J. Med. Chem.* **2016**, *110*, 181–194. https://doi.org/10.1016/j.ejmech.2016.01.023.

(17) Bouckaert, C.; Zhu, S.; Govers-Riemslag, J. W. P.; Depoorter, M.; Diamond, S. L.; Pochet, L. Discovery and Assessment of Water Soluble Coumarins as Inhibitors of the Coagulation Contact Pathway. *Thromb. Res.* **2017**, *157*, 126–133. https://doi.org/10.1016/j.thromres.2017.07.015.

(18) Iversen, P. W.; Beck, B.; Chen, Y.-F.; Dere, W.; Devanarayan, V.; Eastwood, B. J.; Farmen, M. W.; Iturria, S. J.; Montrose, C.; Moore, R. A.; Weidner, J. R.; Sittampalam, G. S. *HTS Assay Validation*; 2004.

(19) Dubský, P.; Ördögová, M.; Malý, M.; Riesová, M. CEval: All-in-One Software for Data Processing and Statistical Evaluations in Affinity Capillary Electrophoresis. *J. Chromatogr. A* **2016**, *1445*, 158–165. https://doi.org/10.1016/j.chroma.2016.04.004.

(20) Altria, K. D.; Kelly, M. A.; Clark, B. J. The Use of a Short-End Injection Procedure to Achieve Improved Performance in Capillary Electrophoresis. *Chromatographia* **1996**, *43* (3–4), 153–158. https://doi.org/10.1007/BF02292944.

(21) Preisler, J.; Yeung, E. S. Characterization of Nonbonded Poly(Ethylene Oxide) Coating for Capillary Electrophoresis via Continuous Monitoring of Electroosmotic Flow. *Anal. Chem.* **1996**, *68* (17), 2885–2889. https://doi.org/10.1021/ac960260s.

(22) Bisswanger, H. *Enzyme Kinetics: Principles and Methods*; Wiley-VCH Verlag GmbH & KGaA: Weinheim, 2008.

(23) Tans, G.; Janssen-Claessen, T.; Rosing, J.; Griffin, J. H. Studies on the Effect of Serine Protease Inhibitors on Activated Contact Factors. Application in Amidolytic Assays for Factor XIIa, Plasma Kallikrein and Factor XIa. *Eur. J. Biochem.* **1987**, *164* (3), 637–642. https://doi.org/10.1111/j.1432-1033.1987.tb11174.x.

(24) Haas, J. V.; Eastwood, B. J.; Iversen, P. W.; Devanarayan, V.; Weidner, J. R. *Minimum Significant Ratio – A Statistic to Assess Assay Variability*; 2004.

(25) Copeland, R. A. *Evaluation of Enzyme Inhibitors in Drug Discovery : A Guide for Medicinal Chemists and Pharmacologists*, Second Edi.; John Wiley & Sons: Hoboken, New Jersey, 2013.

(26) Dementiev, A.; Silva, A.; Yee, C.; Li, Z.; Flavin, M. T.; Sham, H.; Partridge, J. R. Structures of Human Plasma β-Factor XIIa Cocrystallized with Potent Inhibitors. *Blood Adv.* **2018**, *2* (5), 549–558. https://doi.org/10.1182/bloodadvances.2018016337.

(27) Yonetani, T. [26] The Yonetani-Theorell Graphical Method for Examining Overlapping Subsites of Enzyme Active Centers. In *Methods in enzymology*; Academic Press, Inc., 1982; Vol. 87, pp 500–509. https://doi.org/10.1016/S0076-6879(82)87028-6.

(28) Iwata, H.; Oki, H.; Okada, K.; Takagi, T.; Tawada, M.; Miyazaki,

Y.; Imamura, S.; Hori, A.; Lawson, J. D.; Hixon, M. S.; Kimura, H.; Miki, H. A Back-to-Front Fragment-Based Drug Design Search Strategy Targeting the DFG-Out Pocket of Protein Tyrosine Kinases. *ACS Med. Chem. Lett.* **2012**, *3* (4), 342–346. https://doi.org/10.1021/ml3000403.

(29) Backman, T. W. H.; Cao, Y.; Girke, T. ChemMine Tools: An Online Service for Analyzing and Clustering Small Molecules. *Nucleic Acids Res.* **2011**, *39* (suppl), W486–W491. https://doi.org/10.1093/nar/gkr320.

(30) Debela, M.; Magdolen, V.; Grimminger, V.; Sommerhoff, C.; Messerschmidt, A.; Huber, R.; Friedrich, R.; Bode, W.; Goettig, P. Crystal Structures of Human Tissue Kallikrein 4: Activity Modulation by a Specific Zinc Binding Site. *J. Mol. Biol.* **2006**, *362* (5), 1094–1107. https://doi.org/10.1016/j.jmb.2006.08.003.

(31) Burkhard, P.; Taylor, P.; Walkinshaw, M. . An Example of a Protein Ligand Found by Database Mining: Description of the Docking Method and Its Verification by a 2.3 Å X-Ray Structure of a Thrombin-Ligand Complex. *J. Mol. Biol.* **1998**, *277* (2), 449–466. https://doi.org/10.1006/jmbi.1997.1608.

(32) Bajaj, S. P.; Schmidt, A. E.; Agah, S.; Bajaj, M. S.; Padmanabhan, K. High Resolution Structures of P-Aminobenzamidine- and Benzamidine-VIIa/Soluble Tissue Factor. *J. Biol. Chem.* **2006**, *281* (34), 24873–24888. https://doi.org/10.1074/jbc.M509971200.

(33) Jahnke, W.; Erlanson, D. A.; de Esch, I. J. P.; Johnson, C. N.; Mortenson, P. N.; Ochi, Y.; Urushima, T. Fragment-to-Lead Medicinal Chemistry Publications in 2019. *J. Med. Chem.* **2020**, *63* (24), 15494–15507. https://doi.org/10.1021/acs.jmedchem.0c01608.

(34) Melkko, S.; Zhang, Y.; Dumelin, C. E.; Scheuermann, J.; Neri, D. Isolation of High-Affinity Trypsin Inhibitors from a DNA-Encoded Chemical Library. *Angew. Chemie* **2007**, *119* (25), 4755–4758. https://doi.org/10.1002/ANGE.200700654.

(35) Scheuermann, J.; Dumelin, C. E.; Melkko, S.; Zhang, Y.; Mannocci, L.; Jaggi, M.; Sobek, J.; Neri, D. DNA-Encoded Chemical Libraries for the Discovery of MMP-3 Inhibitors. *Bioconjug. Chem.* **2008**, *19* (3), 778–785. https://doi.org/10.1021/BC7004347.

(36) Wichert, M.; Krall, N.; Decurtins, W.; Franzini, R. M.; Pretto, F.; Schneider, P.; Neri, D.; Scheuermann, J. Dual-Display of Small Molecules Enables the Discovery of Ligand Pairs and Facilitates Affinity Maturation. *Nat. Chem. 2015 73* **2015**, *7* (3), 241–249. https://doi.org/10.1038/nchem.2158.

(37) Zimmermann, G.; Neri, D. DNA-Encoded Chemical Libraries: Foundations and Applications in Lead Discovery. *Drug Discov. Today* **2016**, *21* (11), 1828–1834. https://doi.org/10.1016/J.DRUDIS.2016.07.013.

(38) Davis, B. J.; Erlanson, D. A. Learning from Our Mistakes : The ' Unknown Knowns ' in Fragment Screening. *Bioorg. Med. Chem. Lett.* **2013**, *23* (10), 2844–2852. https://doi.org/10.1016/j.bmcl.2013.03.028.

(39) McGovern, S. L.; Helfand, B. T.; Feng, B.; Shoichet, B. K. A Specific Mechanism of Nonspecific Inhibition. *J. Med. Chem.* **2003**, *46* (20), 4265–4272. https://doi.org/10.1021/jm030266r.

(40) Jadhav, A.; Ferreira, R. S.; Klumpp, C.; Mott, B. T.; Austin, C. P.; Inglese, J.; Thomas, C. J.; Maloney, D. J.; Shoichet, B. K.; Simeonov, A. Quantitative Analyses of Aggregation, Autofluorescence, and Reactivity Artifacts in a Screen for Inhibitors of a Thiol Protease. *J. Med. Chem.* **2010**, *53* (1), 37–51. https://doi.org/10.1021/jm901070c.

(41) Shoichet, B. K. Screening in a Spirit Haunted World. *Drug Discov. Today* **2006**, *11* (13–14), 607–615. https://doi.org/10.1016/j.drudis.2006.05.014.

(42) Lewis, L. M.; Engle, L. J.; Pierceall, W. E.; Hughes, D. E.; Shaw, K. J. Affinity Capillary Electrophoresis for the Screening of Novel Antimicrobial Targets. *J. Biomol. Screen.* **2004**, *9* (4), 303–308. https://doi.org/10.1177/1087057104263439.

(43) Gärtner, A.; Ruff, A. J.; Schwaneberg, U. A 96-Multiplex Capillary Electrophoresis Screening Platform for Product Based Evolution of P450 BM3. *Sci. Reports 2019 91* **2019**, *9* (1), 1–11. https://doi.org/10.1038/s41598-019-52077-w.